Room-temperature ferromagnetism observed in Nd-doped In_2O_3 dilute magnetic semiconducting nanowires*

Zhanpeng Lv(吕占朋)[1], Junran Zhang(张军然)[1], Wei Niu(钮伟)[1], Minhao Zhang(张敏昊)[1], Li Song(宋丽)[2], Hairong Zhu(朱海荣)[2], and Xuefeng Wang(王学锋)[1,†]

[1] *Jiangsu Provincial Key Laboratory of Advanced Photonic and Electronic Materials, Collaborative Innovation Center of Advanced Microstructures, School of Electronic Science and Engineering, Nanjing University, Nanjing* 210093, *China*

[2] *Liaoyang Power Supply Branch, Liaoning Provincial Electric Power Corporation Limited, State Grid Corporation of China, Liaoyang* 111000, *China*

(Received 24 May 2016; revised manuscript received 23 June 2016; published online 2 August 2016)

Nd-doped In_2O_3 nanowires were fabricated by an Au-catalyzed chemical vapor deposition method. Nd atoms were successfully doped into the In_2O_3 host lattice structure, as revealed by energy dispersive x-ray spectroscopy, x-ray photoelectron spectroscopy, Raman spectroscopy, and x-ray diffraction. Robust room temperature ferromagnetism was observed in Nd-doped In_2O_3 nanowires, which was attributed to the long-range-mediated magnetization among Nd^{3+}-vacancy complexes through percolation-bound magnetic polarons.

Keywords: dilute magnetic semiconductor, nanowires, ferromagnetism, oxide

PACS: 75.50.Pp, 75.10.−b, 81.15.Gh **DOI:** 10.1088/1674-1056/25/9/097502

1. Introduction

Dilute magnetic semiconductors (DMSs) simultaneously manipulate the degrees of freedom of both the charge and spin of electrons in a single device, which has the potential to revolutionize the current microelectronic devices.[1] In some aspects, the envisioned spintronic devices surpass their counterparts in conventional semiconductor electronics, thus immensely stimulating research efforts in DMSs.[2–12] An intuitively straightforward route toward magnetic semiconductors is to dope the conventional semiconductors to make them ferromagnetic.[13] As an important semiconductor material, In_2O_3 has been widely studied in various fields including semiconductor spintronics. Since Philip *et al.* reported the interesting carrier-controlled above room-temperature ferromagnetism (RTFM) in transparent Cr-doped In_2O_3 thin films,[14] there have been abundant research reports on RTFM in In_2O_3-based DMSs[15–20] as well as in pure In_2O_3.[21] However, most of the research focused on the 3d transition metal (TM) doping,[15–20] where TM ions occupy the corresponding lattice sites in the host with a dilute concentration to minimize the possibility of anti-ferromagnetic ordering.[22]

Compared with TMs with open d shells, 4f rare earth (RE) ions may offer the stronger magnetic interaction and anisotropy and thus may possess the larger magnetic moments in doped semiconductors. However, there have been few research efforts focusing on RE doping in DMSs. Concerning RE-doped In_2O_3, the related research is rather limited. Recently, Xing *et al.* have reported the RTFM in Nd-doped In_2O_3 thin films,[23] but no work on Nd-doped In_2O_3 nanowires has been reported up to now. On the one hand, nanowires stimulate considerable interest due to their miniaturized features as building blocks for future nanoscale spintronic devices. On the other hand, nanowires have the higher aspect ratios and may enhance the ferromagnetic ordering in DMSs.

In this work, we report on the fabrication and properties of Nd-doped In_2O_3 nanowires, which are successfully synthesized by the chemical vapor deposition (CVD) technique. When In atomic sites in the host are substituted by Nd atoms, robust RTFM occurs in Nd-doped In_2O_3 nanowires. The observed RTFM does not come from any experimental artifacts/contaminations. Instead, it is ascribed to the long-range-mediated magnetization among Nd^{3+}-vacancy complexes.

2. Experimental details

Nd-doped In_2O_3 nanowires were grown by a CVD technique, similar to the previous route for the synthesis of Nd-doped ZnO nanowires[3] and Fe-doped In_2O_3 nanowires.[18] Source powders were produced by solid state reaction. Nd_2O_3 (99.995%) and In_2O_3 (99.995%) powders were mixed with alcohol as the weight ratio of 1:4 and milled for 16 h, followed by drying in air at room temperature. The powders were pressed into small pellets, and then sintered at 950 °C for 12 h. This process of milling, pressing and sintering was repeated for three times to achieve homogeneous Nd-doped In_2O_3 powders. To grow the nanowires, the precursor powders and the graphite (99.995%) with a weight ratio of 2:1 were mixed and ground for 60 min, and then loaded into the middle of the quartz tube. Si substrates with 7.5-nm sputtered Au catalysis layers were placed a few centimeters downstream

*Project supported by the National Natural Science Foundation of China (Grant No. 11274003), the Priority Academic Program Development of Jiangsu Higher Education Institutions, China, and the Fundamental Research Funds for the Central Universities, China.

†Corresponding author. E-mail: xfwang@nju.edu.cn

© 2016 Chinese Physical Society and IOP Publishing Ltd

from the source. After the quartz tube was evacuated to a few mTorr, the tube furnace was heated up to 1150 °C at a rate of 10 °C·min^{-1}. During the growth of 150 min, the pressure inside the quartz tube was maintained at ∼ 135 Torr with a constant flow ∼ 200 sccm of Ar and ∼ 2.1 sccm of O_2. After the furnace was cooled to the room temperature, a light gray layer was visible on the surface of the substrates. Care was taken to prevent samples from directly contacting any ferrous tools during preparation. As a control experiment, pure In_2O_3 sample was also prepared under the identical conditions for comparison.

The crystal structure and morphology of the samples were characterized by x-ray diffraction (XRD), scanning electron microscopy (SEM), and transmission electron microscopy (TEM). The doping level and the valence state of Nd ions were determined by x-ray photoelectron spectroscope (XPS) in an ultra-high-vacuum chamber at a pressure lower than 1.0×10^{-9} Torr. Peak positions were referenced to the adventitious C 1s peak taken at 285.0 eV. Raman spectra were recorded at room temperature from a micro-Raman spectrometer (NT-MDT nanofinder-30) with a 514.5-nm Ar^+ laser as an excitation source in the backscattering geometry at room temperature. The magnetic properties were measured by a superconducting quantum interference device (SQUID) magnetometer (Quantum Design MPMS XL-7).

3. Results and discussion

Figures 1(a) and 1(b) show the typical SEM and TEM images of Nd-doped In_2O_3 nanowires, respectively. The diameter of the In_2O_3 nanowires is about 50–200 nm, and the length is about 10–30 μm. The high-resolution transmission electron microscopy (HRTEM) image in Fig. 1(c) shows excellent crystallinity of our samples without any secondary phase. The fast Fourier transform (FFT) pattern of the HRTEM image in the inset further confirms that the Nd-doped In_2O_3 nanowires can be indexed as the expected cubic bixbyite structure. Figure 1(d) presents the XRD patterns of the Nd-doped In_2O_3 nanowires along with the reference sample. Both the undoped and Nd-doped In_2O_3 nanowires exhibit diffraction peaks assigned to cubic bixbyite structure of In_2O_3. No extra diffraction peaks from Nd-related secondary phase or impurities are observed within the sensitivity of XRD. Compared to other diffraction peaks, the intensity of (400) peak is very strong, indicating that all nanowires are highly crystalline and have a good *c*-axis preferred orientation. It is interesting to note that the incorporation of Nd in In_2O_3 leads to the shift of peaks towards the larger angle as compared with that of the undoped In_2O_3 [inset of Fig. 1(d)].

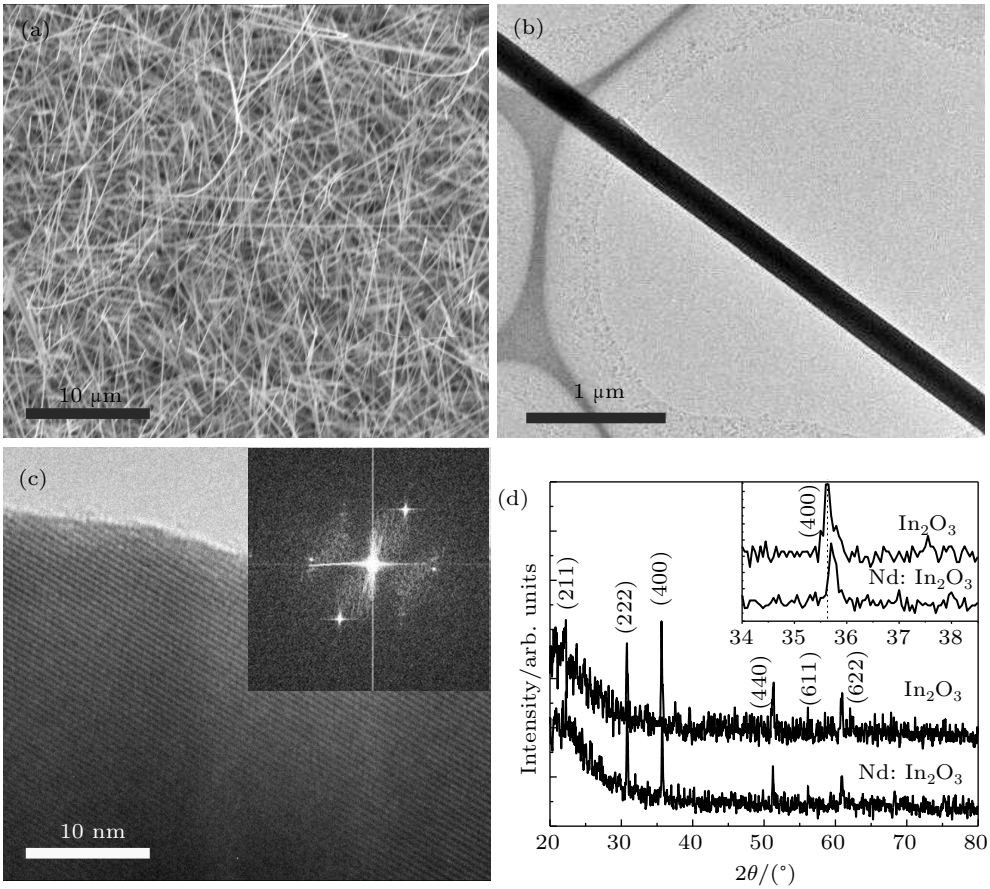


Fig. 1. (a) Typical SEM image of Nd-doped In_2O_3 nanowires. (b) TEM image of a single Nd-doped In_2O_3 nanowire. (c) HRTEM image of a Nd-doped In_2O_3 nanowire. Inset shows the FFT of the HRTEM image, indicating the cubic bixbyite structure of In_2O_3. (d) XRD patterns of pure and Nd-doped In_2O_3 nanowires. Inset is the magnification of the (400) diffraction peak.

To investigate the chemical binding states of the Nd dopant in nanowires, XPS measurements are performed for Nd-doped In_2O_3 nanowires after removing a thin layer via electron bombardment. As shown in Fig. 2(a), only the peaks of In, O, Nd, and C elements are detected. Figures 2(b) and 2(c) show the high-resolution XPS spectra for In 3d and Nd 3d, respectively. In $3d_{5/2}$ and In $3d_{3/2}$ are observed at approximately 443.2 eV and 450.7 eV, respectively. Thus In has valence state of +3, corresponding to the formation of the In_2O_3 phase. The Nd peaks are located at 979.8 eV and 999.6 eV, corresponding to Nd $3d_{5/2}$ and Nd $3d_{3/2}$, respectively.[24] The positions of these peaks indicate that the valence state of Nd is also +3. It is noted that the spectral shape is different from that of Nd_2O_3,[25] suggesting that In should be substituted by Nd. The Nd element is also detected by the energy dispersive x-ray spectroscopy (EDS), as seen from Fig. 2(d). The rough atomic concentration of Nd dopant is about 1.1 at.%, as deduced from EDS result [inset of Fig. 2(d)]. In addition, the atomic ratio of O and In is about 58.74 versus 40.16, smaller than the standard ratio of 3:2. This implies that abundant oxygen vacancies exist in Nd-doped In_2O_3 nanowires, which should actively participate in the electronic structures.

The Raman spectra of In_2O_3 and Nd-doped In_2O_3 nanowires are shown in Fig. 3. In the range of 100–700 cm^{-1} (the silicon Raman signal from substrates is eliminated), six Raman scattering peaks (110 cm^{-1}, 132 cm^{-1}, 306 cm^{-1}, 366 cm^{-1}, 495 cm^{-1}, and 629 cm^{-1}) are observed, and their positions are in agreement with those reported in body-centered cubic In_2O_3 previously.[26] The peak at 132 cm^{-1} is assigned to the In–O vibration of [InO_6] structural units; the peak at 306 cm^{-1} is assigned to the bending vibration of δ-[InO_6] octahedra; the other two peaks 495 cm^{-1} and 629 cm^{-1} are attributed to the stretching vibrations of the same ν-[InO_6] octahedra; whereas the 366 cm^{-1} is assigned to the stretching vibrations of the In–O–In bonds.[27] It can be seen that Nd doping in In_2O_3 leads to the shift of peaks towards the lower frequency (the inset of Fig. 3), as compared to the pure In_2O_3,[26,28] which is attributed to the strain induced by Nd doping.

The key finding of this work is the robust RTFM observed in the In_2O_3 nanowires induced by the intrinsic Nd doping. Figure 4(a) depicts the magnetization versus applied magnetic-field (M–H) curves with clear hysteresis loops after subtracting the substrate contribution measured at 200 K and 300 K, respectively, suggesting the spin–spin coupling-induced ferromagnetic ordering. In contrast, the diamagnetic signal is observed in the undoped sample as indicated in upper inset of Fig. 4(a). In order to exclude the effect of potential

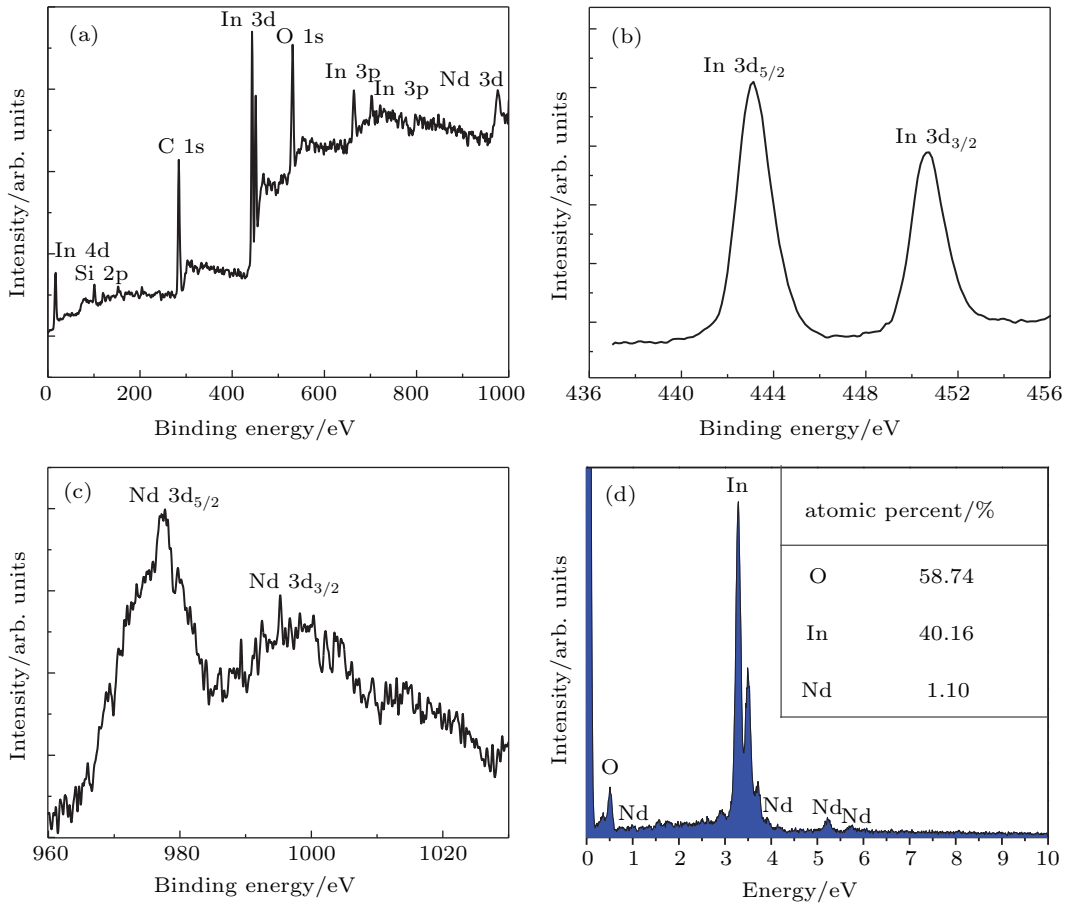


Fig. 2. (color online) (a) XPS survey spectrum of Nd-doped In_2O_3 nanowires. (b) and (c) High-resolution XPS spectra of In 3d and Nd 3d, respectively. (d) EDS spectrum of Nd-doped In_2O_3 nanowires. Inset shows the rough atomic percent of O, In, and Nd.

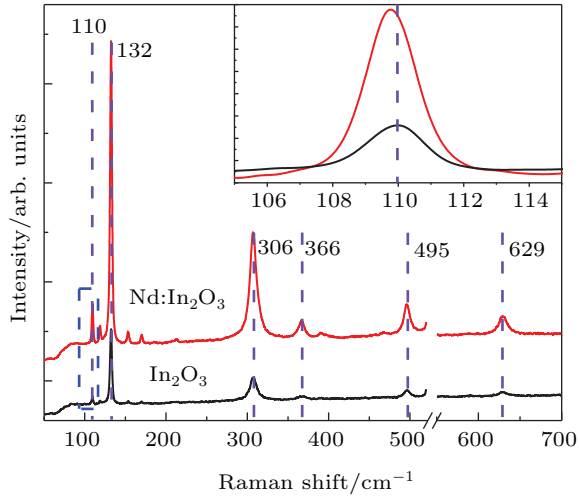


Fig. 3. (color online) Raman spectra of pure In_2O_3 and Nd-doped In_2O_3 nanowires. Inset is the magnification of the dashed rectangular region.

any contamination of the substrates that may contribute to the observed RTFM, we measure the bare silicon substrates following the same procedure and their contributions are determined to be solely diamagnetic. For the Nd-doped In_2O_3 nanowires, the coercive field and the saturation magnetization at 300 K are 100 Oe and 0.12 emu/g, respectively. This saturation magnetization value is roughly 0.1055 μ_B/FU (i.e., μ_B/formula unit), assuming that the distribution of Nd atoms in the In_2O_3 nanowires is uniform and all Nd atoms contribute to the RTFM. Its saturation magnetization value is comparable with that reported by Xing and colleagues in Nd-doped In_2O_3 films.[23] According to the aforementioned structural characterization results as well as the comparison between undoped and doped samples, it is suggested that the observed RTFM in Nd-doped In_2O_3 nanowires is due to the doping effect rather than any ferromagnetic metallic impurities or any other Nd oxidic impurities. Such an intrinsic RTFM in Nd-doped In_2O_3 nanowires is closely associated with the spin coupling of intrinsic defects (i.e., oxygen vacancies) with Nd dopants. In other words, it is believed that an oxygen vacancy in Nd-doped In_2O_3 nanowires can trap one weakly localized electron from the nearby Nd ions. Then the localized carriers will polarize the surrounding magnetic ions of Nd^{3+} to form the magnetic polarons.[29–31] When the density of such magnetic polarons reaches a certain percolation threshold, the overlapping of magnetic polarons will induce the spin–spin interaction between Nd^{3+} ions and vacancies, and eventually establish the long-range ferromagnetic ordering. This elucidation is reasonable in spite of the lack of the direct experimental evidence for the moment. Note that the direct evidence of dopant–vacancy coupling responsible for the RTFM has been reported in Fe-doped In_2O_3 films by resonant inelastic x-ray scattering very recently.[32]

For a better understanding of the RTFM in the Nd-doped In_2O_3 nanowires, we have measured field-cooled (FC) and zero-field-cooled (ZFC) magnetization curves at 500 Oe as a function of temperature, as shown in Fig. 4(b). The result indicates no blocking temperature in the whole temperature range of 5–400 K, suggesting that there should be no tiny contamination of ferromagnetic nanoclusters,[33] consistent with the above results. Moreover, no indication of order–disorder phase transition is observed, indicating the Curie temperature (T_C) higher than 400 K. The discrepancy of T_C between Nd-doped In_2O_3 films ($\sim$ 375 K)[23] and our nanowires is presumably ascribed to the higher aspect ratios of nanowires that may enhance the robust ferromagnetic ordering.

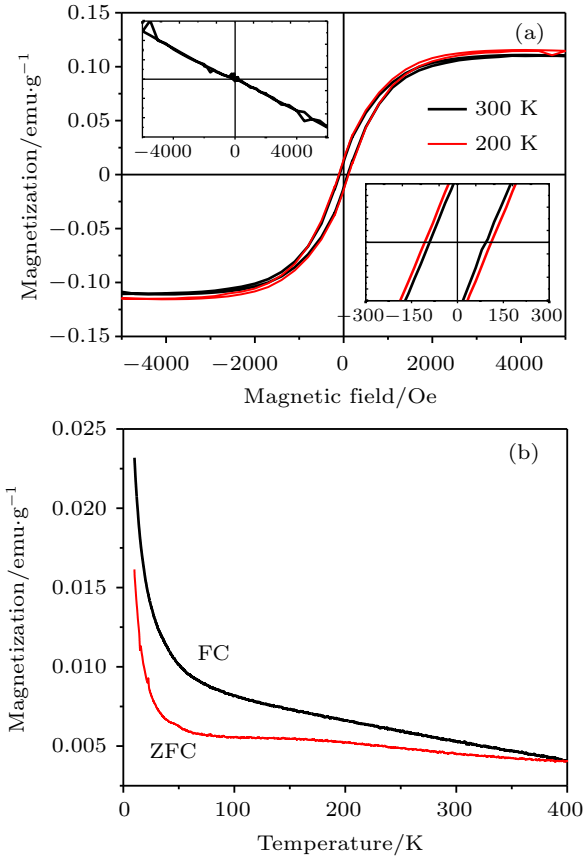


Fig. 4. (color online) (a) Magnetic hysteresis loops of Nd-doped In_2O_3 nanowires at 300 K and 200 K. Upper inset shows the diamagnetic signal of pure In_2O_3 nanowires, and lower inset is the enlargement of loops near the origin. (b) Temperature dependence of ZFC–FC magnetization curves measured at 500 Oe.

4. Conclusion

In summary, we have fabricated Nd-doped In_2O_3 nanowires by a CVD route. Nd-doped In_2O_3 nanowires exhibit a robust ferromagnetic ordering at room temperature. The detailed investigations on the structures demonstrate the high quality of Nd-doped In_2O_3 nanowires without any impurity phases or clusters. The origin of the RTFM is attributed to the long-range-mediated magnetization among Nd^{3+}-vacancy complexes through percolation-bound magnetic polarons. This work will boost the potential applications towards the realization of future nanoscale spintronic devices.

References

[1] Wolf S A, Awschalom D D, Buhrman R A, Daughton J M, von Molnar S, Roukes M L, Chtchelkanova A Y and Treger D M 2001 *Science* **294** 1488

[2] Ogale S B 2010 *Adv. Mater.* **22** 3125

[3] Wang D, Chen Q, Xing G, Yi J, Rahman B S, Ding J, Wang J and Wu T 2012 *Nano Lett.* **12** 3994

[4] Venkatesan M, Fitzgerald C B, Lunney J G and Coey J M D 2004 *Phys. Rev. Lett.* **93** 177206

[5] Degrave J P, Schmitt A L, Selinsky R S, Higgins J M, Keavney D J and Jin S 2011 *Nano Lett.* **11** 4431

[6] Pan D, Wang S L, Wang H L, Yu X Z, Wang X L and Zhao J H 2014 *Chin. Phys. Lett.* **31** 078103

[7] Dietl T and Ohno H 2014 *Rev. Mod. Phys.* **86** 187

[8] Wang X F, Song F Q, Chen Q, Wang T Y, Wang J L, Liu P, Shen M R, Wan J G, Wang G H and Xu J B 2010 *J. Am. Chem. Soc.* **132** 6492

[9] Wang X F, Wan B, Zhang K, Zhao B, Li Z G, Wan X G, Song F Q, Liu B, Xiu X Q, Xu Y B and Zhang R 2013 *J. Phys. Chem. C* **117** 18258

[10] Gong J J, Chen J P, Zhang F, Wu H, Qin M H, Zeng M, Gao X S and Liu J M 2015 *Chin. Phys. B* **24** 037505

[11] Niu W, Zhu H, Wang X F, Ye J D, Song F Q, Zhou J F, Gu S L, Shi Y, Xu Y B and Zhang R 2015 *Appl. Phys. Lett.* **107** 021902

[12] Chou H, Yang K S, Tsao Y C, Dwivedi G D, Lin C P, Sun S J, Lin L K and Lee S F 2016 *Appl. Phys. Lett.* **108** 142404

[13] Ohno H 2001 *Science* **291** 840

[14] Philip J, Punnoose A, Kim B, Reddy K, Layne S, Holmes J, Satpati B, Leclair P, Santos T and Moodera J 2006 *Nat. Mater.* **5** 298

[15] Jiang F X, Xu X H, Zhang J, Fan X C, Wu H S and Gehring G A 2010 *Appl. Phys. Lett.* **96** 052503

[16] An Y, Yang D, Ma G, Zhu Y, Wang S, Wu Z and Liu J 2014 *J. Phys. Chem. C* **118** 10448

[17] Yan S, Qiao W, Zhong W, Au C T and Dou Y 2014 *Appl. Phys. Lett.* **104** 062404

[18] Zhang J R, Wu Z Y, Liu Y J, Lv Z P, Niu W, Wang X F, Du J, Liu W Q, Zhang R and Xu Y B 2015 *Chin. Phys. Lett.* **32** 037501

[19] Nguyen H H, Sakai J, Ngo T H and Brizé V 2005 *Appl. Phys. Lett.* **87** 102505

[20] An Y, Wang S, Duan L, Liu J and Wu Z 2013 *Appl. Phys. Lett.* **102** 212411

[21] Sun S H, Wu P and Xing P F 2013 *Chin. Phys. Lett.* **30** 077503

[22] Kataoka T, Yamazaki Y, Singh V, Fujimori A, Chang F H, Lin H J, Huang D, Chen C, Xing G and Seo J 2011 *Phys. Rev. B* **84** 153203

[23] Xing G Z, Yi J B, Yan F, Wu T and Li S 2014 *Appl. Phys. Lett.* **104** 202411

[24] Selvan R K, Genish I, Perelshtein I, Calderon M J M and Gedanken A 2008 *J. Phys. Chem. C* **112** 1795

[25] Subramanian M, Thakur P, Gautam S, Chae K, Tanemura M, Hihara T, Vijayalakshmi S, Soga T, Kim S and Asokan K 2009 *J. Phys. D: Appl. Phys.* **42** 105410

[26] Meng X, Tang L and Li J 2010 *J. Phys. Chem. C* **114** 17569

[27] Yin W, Su J, Cao M, Ni C, Cloutier S G, Huang Z, Ma X, Ren L, Hu C and Wei B 2009 *J. Phys. Chem. C* **113** 19493

[28] Singhal A, Achary S, Manjanna J, Jayakumar O, Kadam R and Tyagi A 2009 *J. Phys. Chem. C* **113** 3600

[29] Coey J M D, Venkatesan M and Fitzgerald C 2005 *Nat. Mater.* **4** 173

[30] Wang D, Xing G, Yan F, Yan Y and Li S 2014 *Appl. Phys. Lett.* **104** 022412

[31] Wang X F, Xu J B, Zhang B, Yu H G, Wang J, Zhang X X, Yu J G and Li Q 2006 *Adv. Mater.* **18** 2476

[32] Green R J, Regier T Z, Leedahl B, McLeod J A, Xu X H, Chang G S, Kurmaev E Z and Moewes A 2015 *Phys. Rev. Lett.* **115** 167401

[33] Wang X F, Xu J B, Cheung W Y, An J and Ke N 2007 *Appl. Phys. Lett.* **90** 212502